

## Water mass modification in an Arctic fjord through cross-shelf exchange: The seasonal hydrography of Kongsfjorden, Svalbard

Finlo Cottier,<sup>1</sup> Vigdis Tverberg,<sup>2</sup> Mark Inall,<sup>1</sup> Harald Svendsen,<sup>3</sup> Frank Nilsen,<sup>4</sup> and Colin Griffiths<sup>1</sup>

Received 13 October 2004; revised 8 March 2005; accepted 13 July 2005; published 8 December 2005.

[1] Kongsfjorden and the West Spitsbergen Shelf is a region whose seasonal hydrography is dominated by the balance of Atlantic Water, Arctic waters, and glacial melt. Regional seasonality and the cross-shelf exchange processes have been investigated using conductivity-temperature-depth (CTD) observations from 2000–2003 and a 5-month mooring deployment through the spring and summer of 2002. Modeling of shelf-fjord dynamics was performed with the Bergen Ocean Model. Observations show a rapid and overwhelming intrusion of Atlantic Water across the shelf and into the fjord during midsummer giving rise to intense seasonality. Pockets of Atlantic Water, from the West Spitsbergen Current, form through barotropic instabilities at the shelf front. These leak onto the shelf and propagate as topographically steered features toward the fjord. Model results indicate that such cross-front exchange is enhanced by north winds. Normally, Atlantic Water penetration into the fjord is inhibited by a density front at the fjord mouth. This geostrophic control mechanism is found to be more important than the hydraulic control common to many fjords. Slow modification of the fjord water during spring reduces the effectiveness of geostrophic control, and by midsummer, Atlantic Water intrudes into the fjord, switching from being Arctic dominant to Atlantic dominant. Atlantic Water continues to intrude throughout the summer and by September reaches some quasi steady state condition. The fjord adopts a “cold” or “warm” mode according to the degree of Atlantic Water occupation. Horizontal exchange across the shelf may be an important process causing seasonal variability in the northward heat transport to the Arctic.

**Citation:** Cottier, F., V. Tverberg, M. Inall, H. Svendsen, F. Nilsen, and C. Griffiths (2005), Water mass modification in an Arctic fjord through cross-shelf exchange: The seasonal hydrography of Kongsfjorden, Svalbard, *J. Geophys. Res.*, *110*, C12005, doi:10.1029/2004JC002757.

### 1. Introduction

[2] The physical oceanography in the upper layers of Fram Strait is one of balance between northward flowing Atlantic Water, southward flowing Arctic Water and Atlantic Water modified during its circulation through the basins of the Arctic Ocean [Rudels *et al.*, 2000]. On the adjacent shelves, the freshwater input from the glaciers and rivers becomes an additional and important contribution [Meredith *et al.*, 2001]. In particular, the West Spitsbergen Shelf (WSS) is a site where Atlantic, Arctic and glacial waters converge, mix and are exchanged [Saloranta and Svendsen, 2001]. The balance between these three sources of water shifts season by season such that, within an annual cycle,

the shelf waters, and adjacent fjords, switch from a state of Arctic dominance (cold and fresh) to one of Atlantic dominance (warm and saline) and back [Svendsen *et al.*, 2002].

[3] It is widely believed that the effects of global climatic change will be perceptible first, and most acutely, in the polar regions. The hydrographic balance in the shelf regions of the Arctic will be susceptible to changes in oceanic and atmospheric conditions through, for example, variations in the transport of Atlantic Water and glacial discharge. Fjords are commonly regarded as the link between the ocean and the land through cross-shelf exchange and the dynamics of the fjord. The oceanic and terrestrial realms set the fjord boundary conditions, and fjords that actively respond to variations in these conditions may be rather more susceptible to change. Thus the fjords on the west coast of Spitsbergen, which balance Atlantic, Arctic and freshwater inputs, are likely to be sensitive indicators of change.

[4] Although the major effort in studying hydrographic change in Svalbard's fjords has been focused on Storfjorden [Fer *et al.*, 2003; Haarpaintner *et al.*, 2001b; Skogseth, 2003], the Kongsfjorden-Krossfjorden double fjord system in the northwest of Spitsbergen has also been the site of a

<sup>1</sup>Dunstaffnage Marine Laboratory, Scottish Association for Marine Science, Oban, UK.

<sup>2</sup>Polar Environmental Centre, Norwegian Polar Institute, Tromsø, Norway.

<sup>3</sup>Geophysical Institute, University of Bergen, Bergen, Norway.

<sup>4</sup>University Centre in Svalbard (UNIS), Svalbard, Norway.

number of field programs [Hop *et al.*, 2002; Svendsen *et al.*, 2002]. Published observations of conditions on the adjacent WSS are sparse and restricted to summer only [Saloranta and Svendsen, 2001]. The most significant observation related to the hydrography of this region is that it shifts from being Arctic dominant in winter to Atlantic dominant in summer [Svendsen *et al.*, 2002].

[5] While previous studies laid much of the foundation for the local water masses and fjord circulation, they stopped short of a full description of the mechanisms controlling the seasonal cycle of the system. Understanding the processes that determine the chronology, rate and magnitude of the shift from Arctic to Atlantic conditions has implications across many marine disciplines. For example, the accurate interpretation of sediments distribution and palaeo-records [Howe *et al.*, 2003; Koç *et al.*, 2002] and for understanding the composition of biological communities [Basedow *et al.*, 2004; Kwasniewski *et al.*, 2003].

[6] The main objective of this paper is to describe the water masses present in Kongsfjorden and the adjacent shelf and interpret the modification and exchange processes that constitute the massive seasonal changes. We begin with a description of the broad oceanographic features and physiography of the region with particular emphasis on the Kongsfjorden-Krossfjorden system. The data set is introduced followed by a description of the waters masses, their modes of formation, their distribution and the observed hydrographic shift from an Arctic to an Atlantic regime in 2002. The discussion focuses on the mechanisms that control the cross-shelf exchange of water. We also consider the distribution of Atlantic water in the fjord and comment on the interannual response of the system using historical data sets.

## 2. Regional Setting

[7] The Kongsfjorden-Krossfjorden system is located on the northwest coast of Spitsbergen in the Svalbard archipelago (Figure 1a). It is a two-armed fjord system sharing a common mouth located at 79°N, 11°E.

[8] Two source waters dominate conditions west of the common mouth. On the shelf, relatively cold and fresh Arctic Water travels as an anticyclonic coastal current, originating as the East Spitsbergen Current, flowing through Storfjorden, rounding the southern tip of Spitsbergen and northward along the west coast. West of this, on the shelf slope, the relatively saline West Spitsbergen Current (WSC) has been shown to transport great amounts of heat northward, (28 to 45 TW [Schauer *et al.*, 2004], 42 TW [Cisewski *et al.*, 2003] and up to 70 TW [Walczowski *et al.*, 2005]) keeping the waters to the west of the shelf essentially ice free.

[9] Kongsfjorden is oriented from southeast to northwest and is about 20 km long with width varying between 4 and 10 km; refer to Figure 1b. It is partially divided into a series of deep basins, some greater than 300 m, though none have well-defined sills. Krossfjorden is oriented from north to south, about 30 km long and width varying from 3 to 6 km. The outer basins of these two fjords combine at their seaward end to form the main submarine glacial trough, the Kongsfjordrenna, which acts as a deep-water connection across the shelf. A partial sill at the common

mouth runs southward as a submarine spur from the northern peninsular and is apparent in the 200-m contour of Figure 1b.

[10] The communication between fjords and the adjacent shelf is, in general, determined by the topographic features, tidal flow and wind conditions. Other crucial factors that influence the hydrography include the magnitude of freshwater input and the heat fluxes at the surface. Arctic fjords may be regarded as an extreme variant of the “standard” fjord model as they are subject to intense seasonality, very high levels of freshwater input, sea ice formation and melt (reducing surface exchanges), and persistent and strong orographic winds.

[11] At its inner end, Kongsfjorden has five tidewater glaciers draining into it providing the major source of fresh water. Additional sources come from snowmelt, precipitation, run-off and groundwater discharge. The mean annual discharge of fresh water from all these sources into Kongsfjorden is estimated to be about 1.4 km<sup>3</sup> with an annual variation of up to 30% [Svendsen *et al.*, 2002]. Compared to the fjord volume of 29.4 km<sup>3</sup> [Ito and Kudoh, 1997], this climatically sensitive input constitutes about 5% of the mass balance in the fjord. Annual statistics of wind direction show that in Kongsfjorden winds are predominantly down fjord, the next most dominant direction being up fjord [Svendsen *et al.*, 2002].

[12] The internal Rossby radius decreases with increasing latitude such that most Arctic fjords will be wide and rotational effects become important. This is in contrast to many lower latitude fjords that may be regarded as narrow and therefore approximated as simple two-dimensional systems. During summer months when freshwater discharge is maximum, the decoupling between surface and deepwater currents increases because of the strong pycnocline. Under these conditions, Kongsfjorden can be treated as a two-layer system and a rough estimate of the internal Rossby radius of deformation is about 4 km compared to the mean fjord width of 8 km [Svendsen *et al.*, 2002]. As a consequence, Kongsfjorden is strongly affected by rotational dynamics; further evidenced by sediment distributions [Howe *et al.*, 2003].

[13] Ingvaldsen and coworkers [Ingvaldsen *et al.*, 2001] showed by observation and modeling that wind tends to dominate the rotational dynamics of the surface waters in Kongsfjorden and Krossfjorden. Of particular note is the formation of a persistent anticyclonic gyre across the common mouth of the two fjords resulting from interaction between freshwater discharge and relaxation of both up- and down-fjord winds. A synoptic survey with vessel-mounted ADCP across the mouth of Kongsfjorden during summer show that a cyclonic, density driven gyre develops below the surface layer and is indicative of decoupling from the surface waters [Svendsen *et al.*, 2002]. Aspects of these rotational characteristics are reinforced by observations in this study.

## 3. Observations

### 3.1. Mooring Deployments

[14] A single-point mooring was maintained between April and September 2002 at the common mouth of the fjord system in a position 79°3.25'N, 11°18.0'E in 215 m

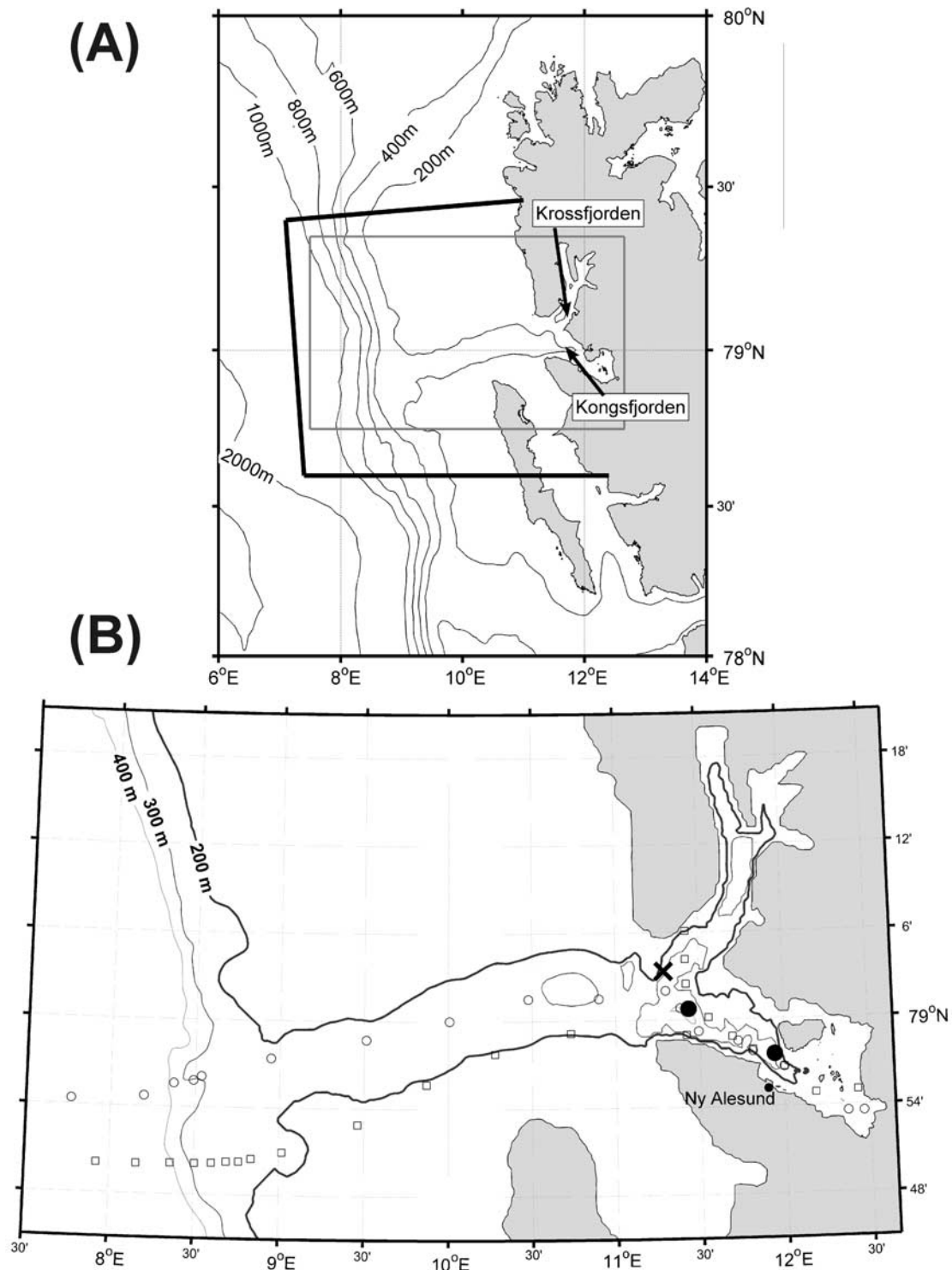


**Figure 1.** (a) Map of the northwest sector of Spitsbergen showing the location of the two fjords, bathymetry of the shelf and shelf slope and the model domain (black line). (b) Expanded view (indicated as the gray line in Figure 1a), showing the positions of CTD stations from surveys in 2002 (open circles, April; open squares, September). Also marked is the mooring location from April to September 2002 (cross) and the two standard CTD K-stations for 2000/2003 (solid circles).

water depth. The mooring location (indicated by cross in Figure 1b) is to the east of the spur extending south from the northern peninsula. The dates of deployment and recovery are summarized in Table 1. On each occasion when the

mooring was deployed or recovered, a CTD profile was obtained.

[15] Instrumentation on the mooring was similar for each deployment and their quantity, depth and sample rates are

**Table 1.** Details of the CTD Profiles Obtained in Kongsfjorden and Adjacent Shelf Between 2000 and 2003

Year	Month	Date	Ship	Station	Duration
2000	September	11	Håkon Mosby <sup>a</sup>	K1	
2001	September	07	Håkon Mosby <sup>a</sup>	K1	
2002	April	14–18	Lance <sup>b,c</sup>	Transect (E/W)	90 hours
		16		Mooring	
	June	16, 14	James Clark Ross <sup>b</sup>	K1/K3	
		23		Mooring	
	July	03	James Clark Ross <sup>b</sup>	Mooring	
		27		Transect (E/W)	
September	28	Håkon Mosby <sup>a</sup>	Transect (N/S)	12 hours	
			28	2 hours	
			27, 29	Mooring	
			28	K1/K3	
2003	August <sup>d</sup>	10, 10	Lance <sup>b</sup>	K1/K3	
	September <sup>d</sup>	04, 04	Lance <sup>b</sup>	K1/K3	

<sup>a</sup>Observations were made with SBE 9 CTD system.

<sup>b</sup>Observations were made with SBE 9/11 + CTD system.

<sup>c</sup>Additional CTD profiles in the inner part of Kongsfjorden were obtained from the fast ice using a miniCTD deployed through the ice.

<sup>d</sup>Profiles from K1 and K3 were obtained within 3 hours of each other in August and within 4 hours in September.

summarized in Table 2. The upward looking 300-kHz ADCP recorded thirty 4-m bins (deepest (145 m), shallowest (29 m)) with standard deviation in velocity of approximately  $0.5 \text{ cm s}^{-1}$ . Salinity measurements from the microcats are accurate to 0.01 salinity units and temperature measurements to  $0.01^\circ\text{C}$ . Miniloggers had a resolution of  $0.1^\circ\text{C}$  (8-bit) and  $0.01^\circ\text{C}$  (12-bit) and accurate to  $0.1^\circ\text{C}$ ; calibrations were checked in a test bath. The two microcats were positioned toward the top and bottom of the mooring and are termed upper and lower respectively. They will be referred to most frequently in this paper with other instruments providing supplementary information.

### 3.2. Hydrographic Data

[16] The CTD data are from ship and ice stations and span the period 2000 to 2003. The locations of stations are indicated in Figure 1b and CTD metadata are summarized in Table 1. In this paper we have made use of CTD profiles from two of the so-called “K” stations (indicated by solid circles in Figure 1b) that form part of the Norwegian Polar Institute and The University Centre in Svalbard standard sampling programs. The most seaward of these, K1, is 6 km south of the mooring position with a water depth of about 340 m. The other, K3, is just north of the settlement of Ny Ålesund in a basin approximately 350 m deep. K1 and K3 are separated by a distance of some 12 km. Profiles from K1 were obtained in September each year during the period

2000–2003. Profiles at K1 and K3 were obtained in August for 2002 and 2003 only.

[17] Two series of CTD stations from the shelf slope to the inner part of Kongsfjorden give complete axial transects of the system running east to west. These stations were occupied in April 2002 (open circles) and September 2002 (open squares). A longitudinal transect was completed in September 2002 across the common mouth. In all cases the CTD data have been calibrated against bottle samples.

### 3.3. Meteorological Data

[18] Wind data were obtained for the fjord from a permanent weather station in Ny Ålesund for the duration of the mooring deployments in 2002. Wind speed and direction recorded every 3 hours were extracted from the database of meteorological observations maintained by the Alfred Wegener Institute.

### 3.4. Model Data

[19] Numerical simulations of the region using the Bergen Ocean Model (BOM) were used as a means of investigating the dynamic interaction between the slope, shelf and fjord thereby aiding interpretation of the observational data. This primitive equations, sigma-coordinate ocean model assumes Boussinesq and hydrostatic approximation and solves for the barotropic field at higher resolution in time than the baroclinic field [Berntsen, 2000]. It was set up for the

**Table 2.** Details of the Instrumentation Included on Each Mooring Deployment<sup>a</sup>

Instrument	Quantity	Depth, m	Sample Interval
<i>Deployment 1</i>			
Seabird microcat	2	40, 205	4 min
Minilog, 8 bit	4	30, 65, 150, 175	16 min
Minilog, 12 bit	6	35, 55, 70, 100, 120, 155	12 min
RDI 300-kHz ADCP	1	150	4 min (33 ppe)
24-bottle sediment trap	1	65	3.5 days/bottle
<i>Deployment 2</i>			
Seabird microcat	2	45, 205	4 min
Minilog, 8 bit	3	30, 35, 55	16 min
Minilog, 12 bit	6	70, 120, 130, 150, 180, 205	12 min
RDI 300-kHz ADCP	1	150	4 min (33 ppe)
24-bottle sediment trap	1	65	3.5 days/bottle

<sup>a</sup>The table includes the number of instruments, their depth from the surface, and the sampling interval for each.

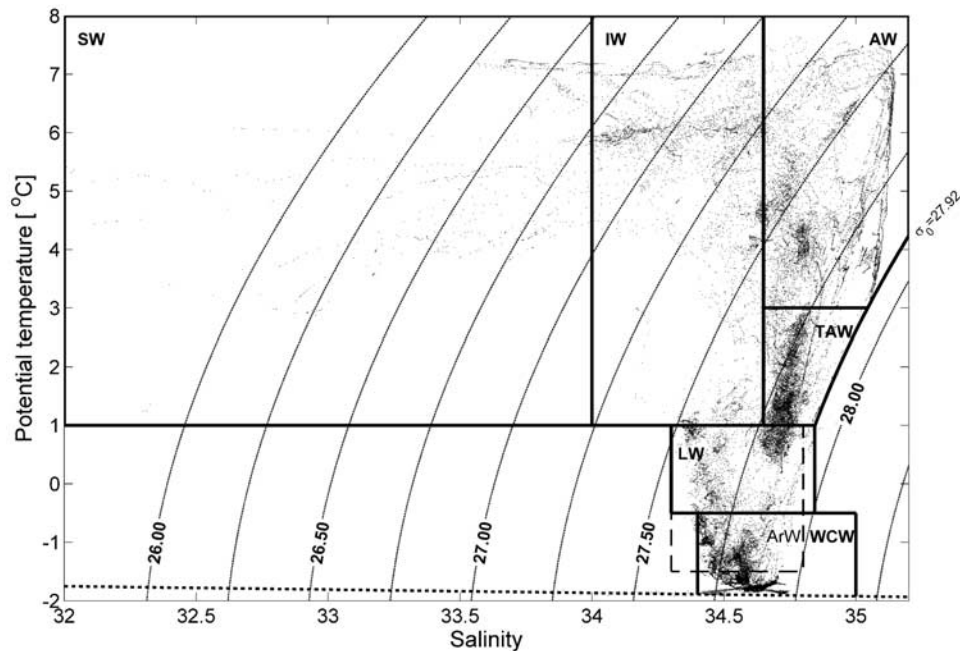


**Figure 2.** T-S diagram for the water masses that have been found to be resident in the Kongsfjorden and adjacent shelf region adapted from a classification scheme of *Svendsen et al.* [2002]. All data used in this paper are plotted on the diagram. External water masses are Atlantic Water (AW) and Arctic Water (ArW); internal water masses are Winter Cooled Water (WCW), Local Water (LW), and Surface Water (SW); water masses of mixed origin are Transformed Atlantic Water (TAW) and Intermediate Water (IW). Water mass definitions are identical to those listed in Table 3. Isopycnals are at 0.25 intervals, and the dotted line indicates the freezing point.

Kongsfjorden-Krossfjorden system and adjacent shelf and shelf slope, with a  $500 \text{ m} \times 500 \text{ m}$  resolution grid domain, on the basis of the International Bathymetric Chart of the Arctic Ocean (IBCAO) in the coastal area, and Norwegian charts in the fjords. The zonal  $\times$  meridional domain size covers  $218 \times 174$  grid cells, giving a domain size  $108.5 \times 86.5 \text{ km}$ , with 32 sigma-layers in the vertical. The extent of the model domain is illustrated in Figure 1a.

[20] Tidal forcing is imposed as a surface elevation boundary condition along the western boundary using four tidal constituents calculated from tidal measurements in Kongsfjorden (M2, S2, N2 and K1). This gives good stability to the barotropic wave response of the model in a region of steep topography and reproduces well the characteristics and propagation of the barotropic tide in the fjord. Wind forcing uses a wind field taken from the hindcast database of the Norwegian Meteorological Institute; model estimates of wind speed from observed pressure fields giving a time resolution of 6 hours and a spatial resolution of 75 km. An adjustment is made to the geostrophic wind field within the fjords to account for the orographic effects on direction and somewhat reduced wind speeds. Although real winds are used in the model it is not intended to be operated as a hindcast simulation of T-S evolution in the region.

[21] The initial temperature and salinity fields were estimated using data from a semi-synoptic hydrographic survey of the region in April 2002. A geostrophically balanced barotropic slope current was imposed in the initial velocity and surface elevation fields. Boundary conditions of temperature, salinity, velocity and surface elevation were

imposed along all lateral boundaries using a Flow Relaxation Scheme (FRS) [Martinsen and Engedahl, 1987]. Boundary conditions along the southern and western boundaries were taken from the initial fields. Along the northern boundary the boundary conditions were calculated from a five-cell average south of the relaxation zone to permit a free flow of water masses out of the domain.

## 4. Results and Analysis

### 4.1. Water Mass Classification

[22] Previous descriptions of water masses within the fjord [Ito and Kudoh, 1997] have been rather unsatisfactory with respect to the likely exchange mechanisms. The most recent classification [Svendsen et al., 2002] identifies a number of distinct water masses that are consistent with a cross-shelf exchange mechanism and has proved useful in the interpretation of biological observations [Basedow et al., 2004; Kwasniewski et al., 2003]. In this paper, we will use the Svendsen classification making refinements to it where appropriate. We continue by describing the origins, or modes of formation, of each water mass. The domain each occupies in T-S space is shown in Figure 2, which is overlain by all data used in this paper; their definitions are given in Table 3.

[23] The two principal water masses originating outside the fjord are the Atlantic Water (AW) in the WSC and the Arctic-type water (ArW) in the coastal current. Both currents flow northward, the former following the shelf slope and the latter on the shelf, and are separated by a frontal region. In the summer, this may exist as a temperature and

**Table 3.** Definitions for Water Masses Found in Kongsfjorden and on the Adjacent Shelf<sup>a</sup>

Water Mass	Abbreviation	Characteristic		
		T (°C)	S	$\sigma_\theta$
External				
Atlantic water	AW	>3.0	>34.65	<27.92
Arctic water	ArW	−1.5 to 1.0	34.30 to 34.80	
Internal				
Winter-cooled water	WCW	<−0.5	34.40 to 35.00	
Local water	LW	−0.5 to 1.0	34.30 to 34.85	
Surface water	SW	>1.0	<34.00	
Mixed				
Transformed Atlantic water	TAW	1.0 to 3.0	>34.65	<27.92
Intermediate water	IW	>1.0	34.00 to 34.65	

<sup>a</sup>These domains are represented in the T-S diagram of Figure 3.

salinity front [Saloranta and Svendsen, 2001] while CTD data from April 2002 show there is also a density front in early spring.

[24] AW is the warmest and most saline, usually defined as  $T \geq 3^\circ\text{C}$  and  $S \geq 34.9$  [Manley, 1995]; though the salinity minimum is taken as low as 34.65 in areas north-west of Spitsbergen through mixing with fresh polar surface waters [Rudels et al., 2000]. We adopt this lower salinity boundary. ArW is colder and fresher than AW and is further freshened as it moves northward due to the outflow from adjacent fjords. It is a heavily modified extension of the East Spitsbergen Current (ESC) with a much wider range of salinities than quoted for ESC [Haarpaintner et al., 2001b; Skogseth, 2003].

[25] Much of the AW entering Kongsfjorden mixes with ArW as it crosses the shelf. As a result, it differs significantly from the water in the core of the WSC and can be regarded as distinct. This Transformed Atlantic Water (TAW) lies on a mixing line between AW and ArW. Throughout the remainder of this paper, the term Atlantic Water will refer to any water of Atlantic origin (AW and TAW) whereas the abbreviations AW and TAW will refer to the distinct domains in the T-S diagram.

[26] Surface Water (SW) forms from glacial melt and is dominant in late spring and summer in a layer that generally decreases toward the fjord mouth [Svendsen et al., 2002]. Its wide temperature range is due to the high particulate content which promotes warming by insolation. In general, the salinity of SW varies from 34 to less than 28 close to the glaciers; the lower boundary of 32 in Figure 2 is not indicative of a minimum salinity. Entrainment and mixing at the boundary of SW with underlying AW or TAW is the mechanism for forming Intermediate Water (IW).

[27] During the autumn and winter, two water masses are formed in the fjord through surface cooling and convection. Local Water (LW) is generally of low temperature ( $<1.0^\circ\text{C}$ ) with a salinity range dependent on the water present in the fjord at the end of the summer. Sea ice formation and associated convection during intense cooling produces very cold and dense Winter Cooled Water (WCW). This is analogous to the formation of a dense outflow in Storfjorden [Haarpaintner et al., 2001a; Quadfasel et al., 1988; Skogseth et al., 2004]. WCW can be found throughout Kongsfjorden at the end of winter and is also detected throughout the year at the bottom of deep basins and depressions. Gradual warming and freshening of LW and WCW in spring and early summer through mixing with

the surface waters can modify their T-S signatures toward that of IW. Consequently, IW is formed through two distinct processes depending on the time of year and the occurrence of particular water masses.

#### 4.2. Cross-Shelf CTD Survey

[28] The key observations motivating this paper were two CTD surveys completed in April and September 2002 extending from the shelf slope to the inner basin of Kongsfjorden along the main axis of Kongsfjordrenna. The temperature, salinity and density distribution for April and September are presented in Figures 3a–3c and 4a–4c, respectively. Occurrence of AW in each section is indicated by the gray shaded region. The key contrast between the two surveys is the massive change in the quantity of AW present on the shelf and in the fjord from April to September.

[29] In April, AW was found over the shelf slope in the core of the WSC from the surface down to 300 m and close to the slope surface. Eastward of this core was an intense frontal region with strong horizontal gradients and near vertical isotherms and isohalines. Sloping isopycnals to the west of the core are consistent with a northward geostrophic flow and the reverse slope of isopycnals to the east is indicative of Ekman drainage off the shelf, further evidenced by the deviation in the isotherms and isohalines close to the shelf slope. On the shelf, northward flowing ArW is dominant and within this are two pockets of Atlantic Water (recognizable by a rather higher temperature and salinity than the surrounding water) that have penetrated the front. There is little evidence of these pockets in the density field.

[30] The horizontal isopycnals in Figure 3c show that there are very weak geostrophic flows on the shelf. In contrast, within the fjord the isopycnals are generally sloping. Density fronts at the mouth mark the transition to the relatively isothermal conditions inside the fjord. At this time, Kongsfjorden was filled with WCW and weakly stratified ( $\Delta\rho \approx 0.2 \text{ kg m}^{-3}$  over the upper 200 m) by a vertical salinity gradient, presumably due to the continual supply of fresh water from the temperate layers in the surrounding glaciers.

[31] The sections from the CTD survey in September of 2002, Figures 4a–4c, illustrate the considerable occupation by AW throughout the section. The top of the AW layer is at about 40 m extending to below 400 m on the shelf slope and to about 250 m in the entrance to the fjord. Throughout the section the AW layer is capped by considerably cooler and

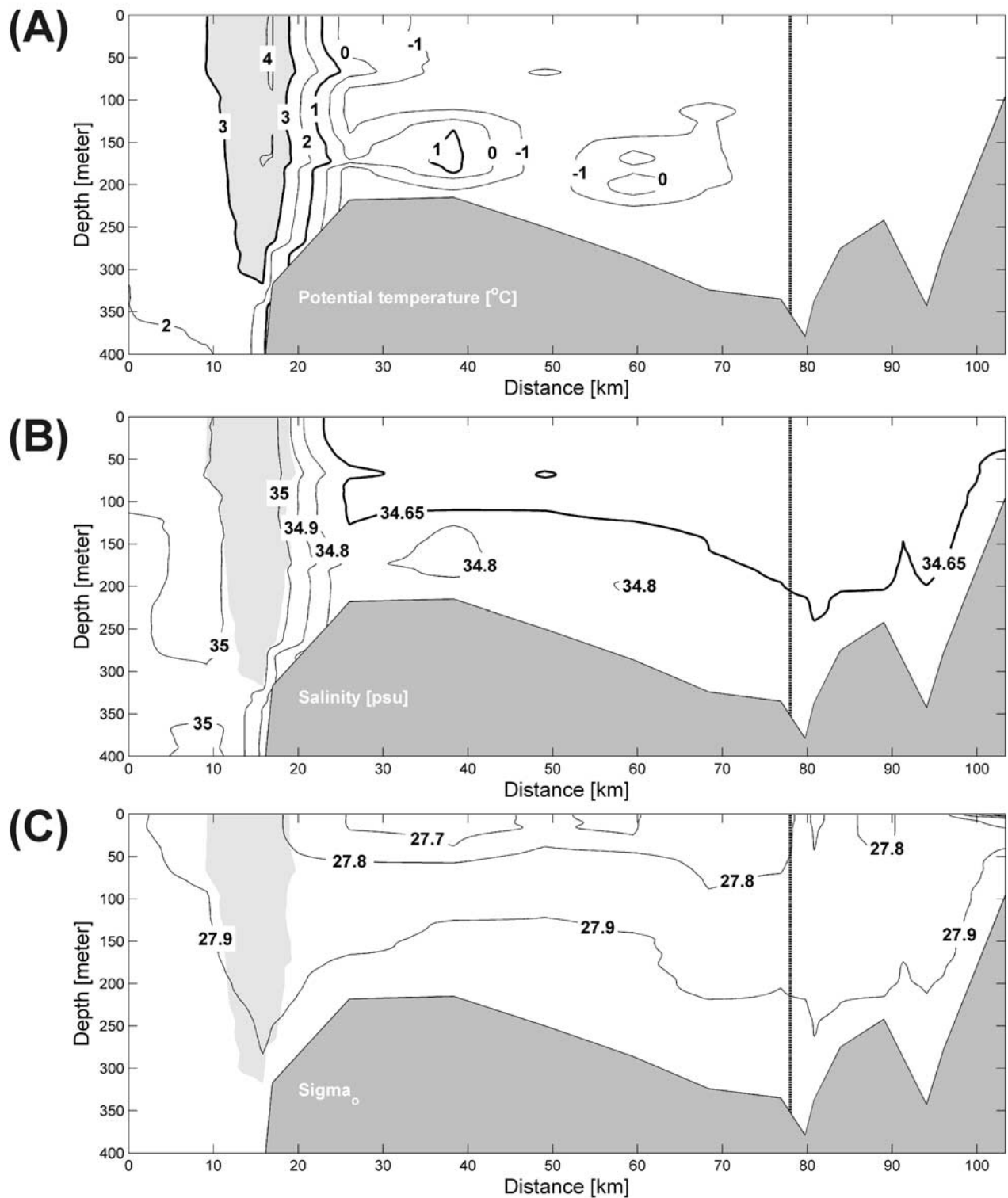


**Figure 3.** (a) Temperature, (b) salinity, and (c) density sections from April 2002. The survey is from the shelf slope along Kongsfjordrenna and into Kongsfjorden with the corresponding CTD stations marked as open circles in Figure 1b. The vertical dotted line marks the mouth of the fjord and the pale gray shaded area in each section indicates the extent of AW. Isolines are drawn at (Figure 3a)  $-1^{\circ}\text{C}$  to  $4^{\circ}\text{C}$  in  $1^{\circ}\text{C}$  steps, (Figure 3b) 34.65, 34.80 to 35.10 in 0.1 steps, and (Figure 3c) 27.7 to 27.9 in 0.1 steps. Thick isolines correspond to water mass boundaries; refer to Table 3.

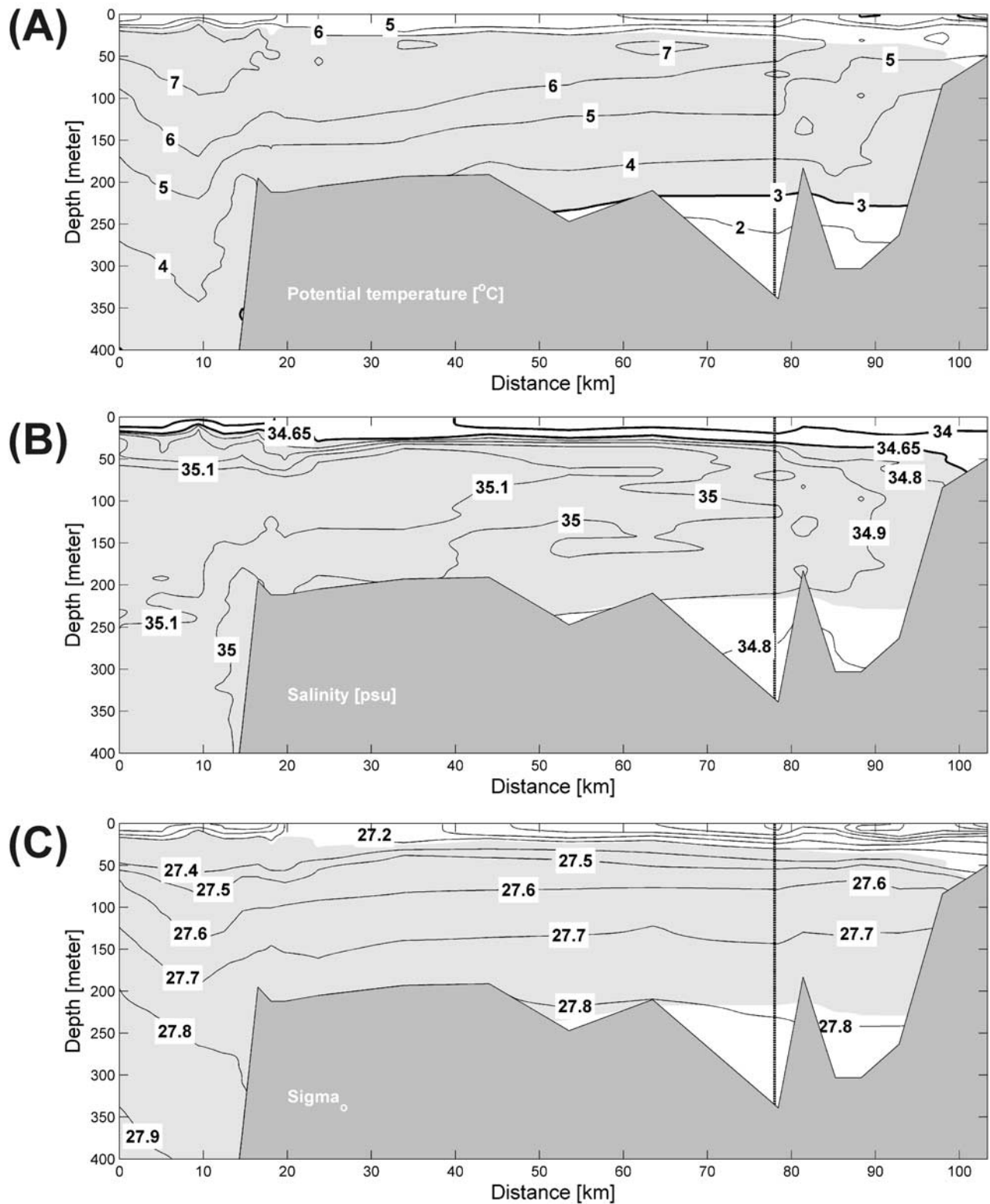


**Figure 4.** (a) Temperature, (b) salinity, and (c) density sections from September 2002. The survey is from the shelf slope along Kongsfjordrenna and into Kongsfjorden with the corresponding CTD stations marked as open squares in Figure 1b. The vertical dotted line marks the mouth of the fjord, and the pale gray shaded area in each figure indicates the extent of AW in the section. Isolines are drawn at (Figure 4a) 2°C to 7°C in 1°C steps, (Figure 4b) 34.00, 34.65, 34.80 to 35.10 in 0.1 steps, and (Figure 4c) 26.0 to 27.4 in 0.2 steps and 27.4 to 27.9 in 0.1 steps. Thick isolines correspond to water mass boundaries; refer to Table 3.



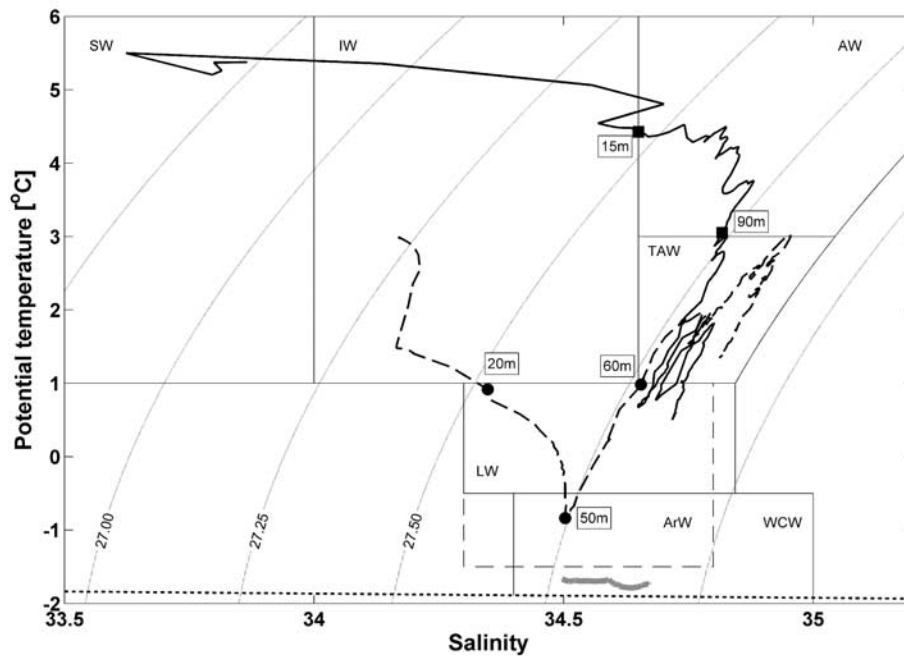


**Figure 5.** T-S distribution for three CTD profiles taken at the mooring location in April (thick gray line), June (dashed black line), and July (solid black line) 2002. Depth points for June (solid circles) and July (solid squares) are added.

fresher meltwater and in the fjord pockets of TAW are retained in depressions below the AW.

[32] In contrast to April and to previous observations of cross-shelf hydrography [Saloranta and Svendsen, 2001], there is no evidence of a salinity front at the shelf break and only very weak temperature and density fronts on the shelf slope. The inclination of the isopycnals at the shelf slope is much reduced indicating weaker northward geostrophic flow. On the shelf and in the fjord, isopycnals are horizontal and parallel though the vertical density gradients are very much greater than for April, typically  $\Delta\rho \approx 1.2 \text{ kg m}^{-3}$  over the upper 200 m.

### 4.3. Mooring Hydrography

#### 4.3.1. Residual Currents

[33] ADCP data show that currents are rather complex and variable in the vicinity of the mooring. Daily averaged residual currents were calculated after removing the dominant diurnal and semidiurnal constituents. Through both deployment periods the residual flow in water deeper than 100 m was directed between south and south-southwest with mean magnitudes of 3.7 and 3.0  $\text{cm s}^{-1}$  for the two periods. In the deepest bins the Neumann's steadiness factor [Souza et al., 2001] was greater than 0.7, where a completely steady flow corresponds to a value of 1.0. This compares with values between 0.5 and 0.9 found for topographically steered slope currents [Souza et al., 2001]. This remarkably persistent flow is consistent with the mooring located in the northwest quadrant of a cyclonic gyre as reported by Svendsen and others [Svendsen et al., 2002] and also a steering effect by the adjacent spur.

[34] In water shallower than 80 m, steadiness was less than 0.2. Residual current directions at 60 m during the first deployment were distributed uniformly while those during

the second deployment had a pronounced bimodal distribution with the modes separated by approximately  $180^\circ$ . The bimodal distribution implies both cyclonic and anticyclonic gyres occurring in the fjord mouth due to greater decoupling of the surface from deeper waters as freshwater discharge increases during the summer.

[35] These observations reinforce previous descriptions of flow in Kongsfjorden, particularly regarding the occurrence of basin-scale gyres [Ingvaldsen et al., 2001; Svendsen et al., 2002]. The transit time around the gyre of distance 15 km is about 3–4 days, consequently, the observations at the mooring must be interpreted with due regard for the inherent time lag due to advection and the potential for modification during the transit.

#### 4.3.2. CTD Data

[36] The CTD sections of April and September 2002 illustrate the considerable shift in the shelf and fjord hydrography. Stages in this shift are captured in the CTD profiles obtained at the mooring position in April, June and July 2002, the data from which are plotted on the T-S diagram in Figure 5. Depth indicators are added to aid description.

[37] In April the water is relatively homogeneous, weakly stratified and tightly constrained in the WCW domain close to the freezing point line. The CTD sections in Figure 3 reinforce the assumption that the entire fjord exists in a homogeneous state at this time. Data from 23 June show that there has been considerable modification and intrusion of water masses into the fjord mouth. Atlantic water is now present with TAW occupying the intermediate and deep water from 60 m to the bottom. Above this, concentrated at 50 m, are remnants of WCW and above 20 m is IW formed from WCW that has warmed and freshened through mixing.

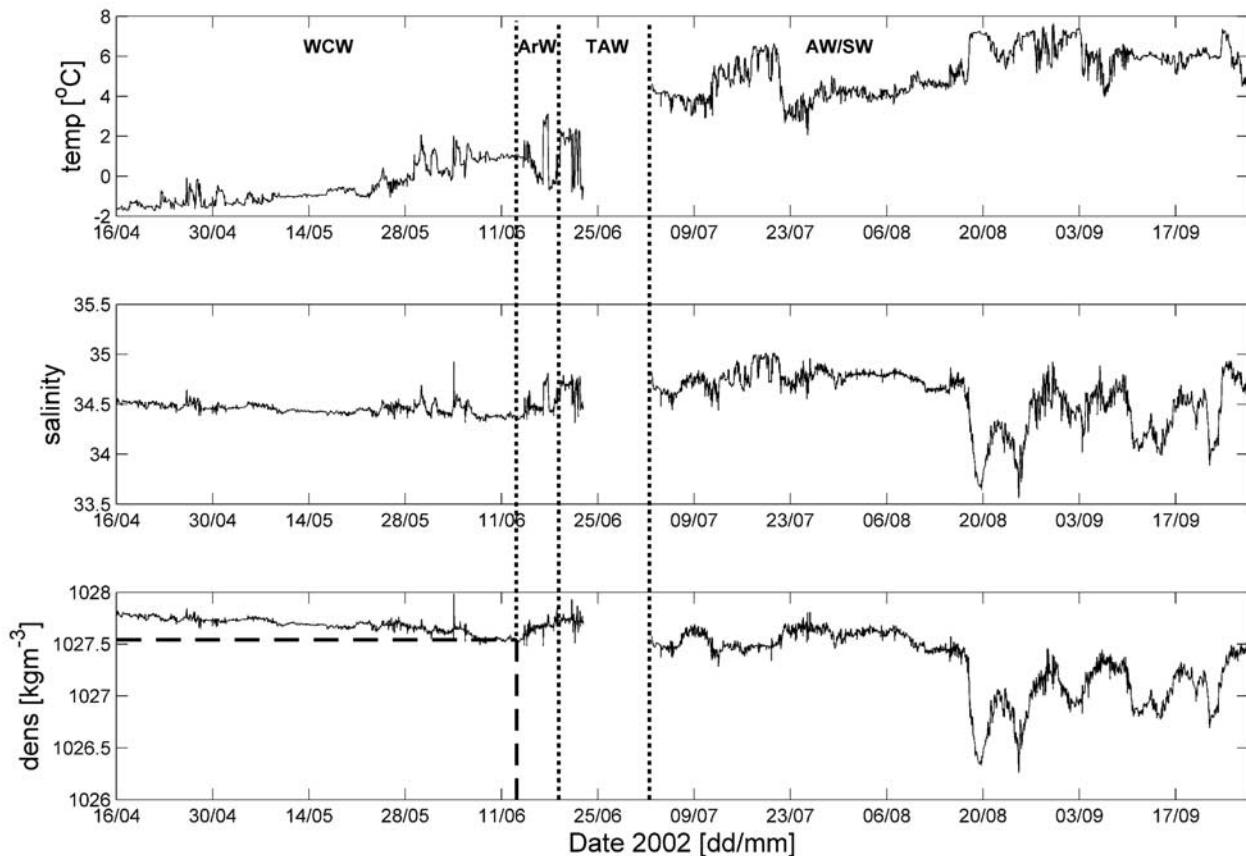


**Figure 6.** Time series of temperature, salinity, and density recorded by the upper microcat on the mooring in 40 m depth during 2002. The vertical dotted lines indicate the demarcation between periods of occupation by individual water masses, and the dashed line in the bottom panel marks the time and density of the first change in water mass.

[38] Data from 3 July illustrate the rapid and substantial hydrographic change that occurred in the intervening 11-day period. AW occupies the water column between 15 m and 90 m, replacing the highly modified WCW in the upper layers. A thin layer of SW lies above the AW, separated by a very strong halocline. The predominant water mass extending from the base of the AW layer toward the bed is TAW. Interleaved with the TAW and at the bottom are cold layers of relatively high salinity water reminiscent of modified WCW. It is reasonable to speculate that the source of the interleaved WCW is an outflow from inner parts of the fjord caused by inflow of AW at intermediate depths. Water with the appropriate T-S properties for modified WCW was identified in CTD data from station K3 in June (data not presented).

#### 4.3.3. Time Series

[39] The CTD data show a clear shift from conditions where WCW dominated to one where AW dominated. It is also clear from Figure 5 that there was substantial intrusion of AW into Kongsfjorden in the period when the mooring was being serviced. Although the mooring did not capture the dynamics of this particular intrusion, it did record the change in the in the weeks either side. The T-S diagram in Figure 2 shows that temperature alone is far from adequate for interpreting the changing water masses. Consequently, the main sources of T-S data for monitoring change at the

mooring location were the two Seabird microcats located at depths of 40 and 205 m. These instruments were not pumped, so there was a tendency for the salinity record to become spiky, which was translated into to the density data. A simple median despiking routine was applied.

#### 4.3.3.1. Upper Microcat

[40] Time series of temperature, salinity and density for the upper microcat are shown in Figure 6. The gap in the data at the end of June marks the period when the mooring was serviced and vertical dotted lines indicate demarcation between different water masses. The data show a gradual warming and freshening of WCW through April and May with the density decreasing at a mean rate of  $3 \times 10^{-3} \text{ kg m}^{-3} \text{ d}^{-1}$  to 13 June. This slow modification is most likely through vertical mixing of warmer and fresher surface water.

[41] By 28 May there are times when T-S signature of the water corresponds that of ArW. The relatively rapid change in temperature suggests some limited exchange of WCW with ArW in the upper part of the water column. During June, the steady, long-term changes in temperature and salinity are punctuated by rapid deviations in both parameters. These are interpreted as pockets of ArW interleaving with the modified WCW indicating that the mooring position lay close to the front between the predominantly WCW in the fjord and the ArW on the shelf. The first

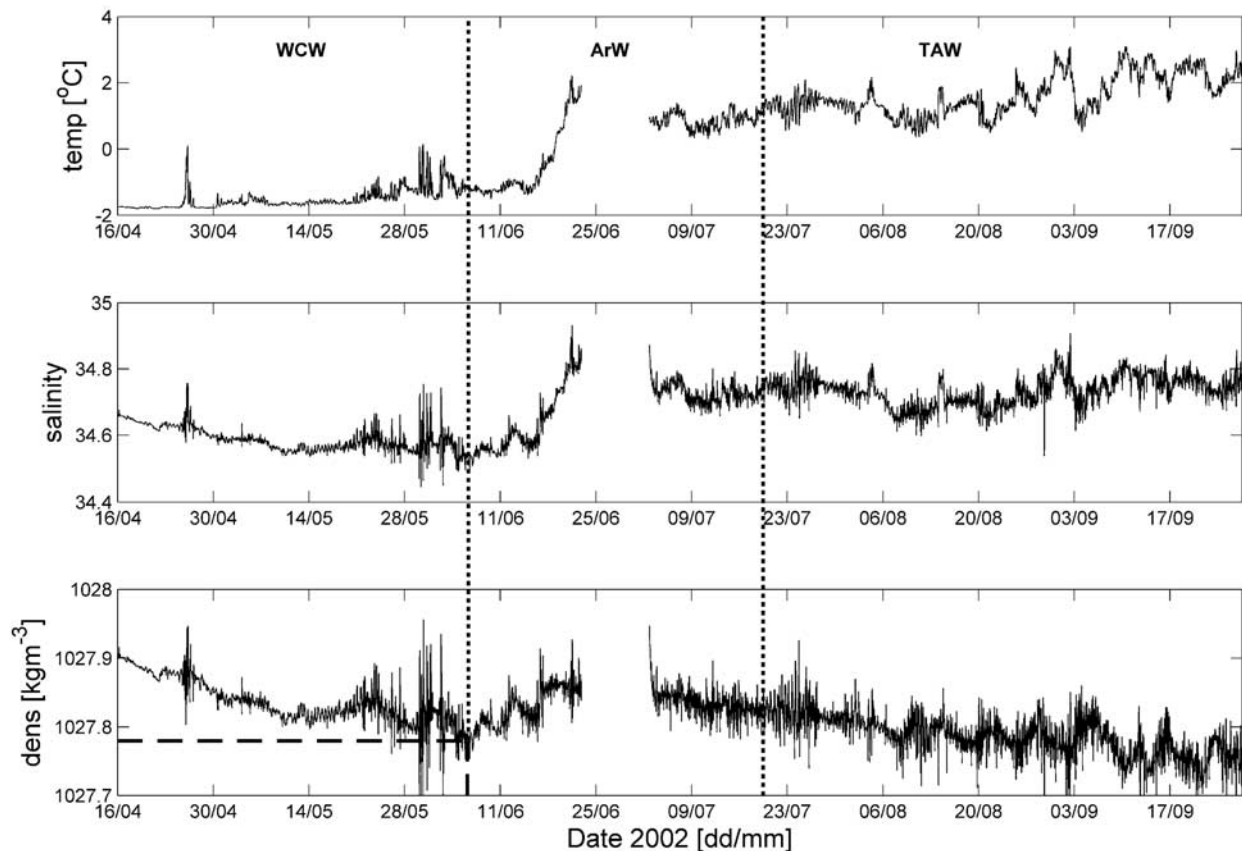


**Figure 7.** Time series of temperature, salinity, and density recorded by the lower microcat on the mooring in 205 m depth during 2002. The vertical dotted lines indicate the demarcation between periods of occupation by individual water masses, and the dashed line in the bottom panel marks the time and density of the first change in water mass.

significant changes in T-S properties occur on 13 June with a rapid decrease in temperature. This is interpreted as an exchange of water with ArW replacing the modified WCW. There is further change on 19 June with rapid increases in both temperature and salinity corresponding to occupation by TAW at 40 m.

[42] In the period when the mooring was being serviced there was a shift from TAW to AW with temperature increasing by  $5^{\circ}\text{C}$  and salinity by 0.2 with a concomitant decrease in density. AW then dominated the upper part of the water column until 18 August when the T-S characteristics oscillated between AW and SW with rapid and large salinity changes of about 1 salinity unit in 24 hours.

#### 4.3.3.2. Lower Microcat

[43] The T and S data from the lower microcat is presented in Figure 7. Through April and May, there was a gradual increase in temperature and a decrease in salinity of the WCW. Similarly to the upper microcat the steady change was punctuated by small and brief deviations, again indicative of pockets of ArW within the WCW. The rate of decrease in density between 16 April and 7 June was  $2 \times 10^{-3} \text{ kg m}^{-3} \text{ d}^{-1}$ , slightly less than that measured at the upper microcat and consistent with classical behavior of fjordic deep water. The differing rates of density change measured at the microcats resulted in the stratification in June being three times that in April.

[44] From 7 June, both temperature and salinity begin to increase, progressing very rapidly after 15 June until the mooring was removed. This change is associated with a transition from WCW to predominantly ArW with occurrence of TAW at the end of the deployment. On redeployment the characteristics of the deep water were clearly those of ArW and persisted until 20 July when there was long-term occupation by TAW. At no time during the mooring deployment was AW present in the deep water.

[45] The steady changes observed at each microcat during the first deployment are indicative of diffuse mixing through the entire water column. There are two factors that may have facilitated this. First, there was no strong pycnocline to inhibit vertical mixing throughout April and May. Second, the residual currents flowing parallel to the steep-sided spur running out from the northern peninsular will generate some degree of boundary-like mixing of the bottom water in the area close to the mooring.

## 5. Discussion

[46] The principal observation from the hydrographic data presented above is the rapid and extensive intrusion of Atlantic Water across the shelf and into the fjord. Here we discuss the possible causes of the massive hydrographic shift and the mechanism that controls the cross-shelf exchange.

The discussion also includes analysis of the extent of, and interannual variations in, the occupation by AW in Kongsfjorden.

[47] Ignoring the observed salinity changes entirely, a very simplistic argument for the cause of the large temperature change is that it is purely the result of solar heating of the surface waters and efficient vertical mixing. It is clear from Figure 5 that there was substantial net heat gain in the upper half of the water column. The vertically integrated heat content  $H$ , at the mooring position was calculated from the June and July CTD profiles using a reference temperature and salinity for WCW of  $-1.7^{\circ}\text{C}$  and 34.6, respectively. The difference between the two values,  $\Delta H$ , is the change in heat content during the 11 days between CTD casts.

[48] Over the full depth,  $\Delta H = 7.8 \times 10^8 \text{ J m}^{-2}$ , necessitating a net surface heat flux during the 11 days of  $820 \text{ W m}^{-2}$ , assuming this change was the result of surface fluxes alone. Monthly mean atmospheric heat fluxes at position  $79.5^{\circ}\text{N}$ ,  $10.5^{\circ}\text{E}$  were calculated using estimates of heat flux between 1980 and 1998 taken from the Southampton Oceanography Centre climatological atlas [Josey *et al.*, 1999]. The values for June and July are  $46.8 \text{ W m}^{-2}$  and  $66.8 \text{ W m}^{-2}$ , respectively, giving a weighted mean over the 11-day period of  $52 \text{ W m}^{-2}$ , an order of magnitude less than the heating required. This confirms that the increase in heat content is due principally to advection of a warm water mass across the shelf and into the fjord.

### 5.1. Cross-Shelf Exchange Mechanism

[49] It is important to recall that AW is present on the shelf slope in the WSC year round and that the CTD section of April 2002, Figure 3, suggests that it tends to leak across the front and onto the shelf. Also, the mooring data show the substantial and relatively rapid change in water masses in the fjord at approximately midsummer with locally produced WCW being replaced by AW originating from the WSC. However, the critical aspect of these observations is that despite the seemingly continuous proximity of AW, it does not occupy the fjord until a particular combination of conditions on the shelf and at the fjord mouth is satisfied.

[50] An essential first step is to explain how the AW penetrates the front. It has been proposed, based on observations of the frontal structure across the WSS, that the front between AW and ArW is susceptible to barotropic instabilities [Saloranta and Svendsen, 2001]. These instabilities in the front then break away to create pulses of AW that propagate onto the shelf. Support for this mechanism comes from both observations of the WSC and output from BOM.

[51] The WSC is topographically steered along the shelf slope following isobaths. Vessel-mounted ADCP sections in the shelf area have demonstrated the unidirectional property of the currents and also lateral shear in the flow [Knutsen, 2003]. The barotropic nature of the WSC [Fahrbach *et al.*, 2001] makes it responsive to surface winds which if blowing to the north or south will tend to move water by Ekman transport up or down the slope. Applying the conservation of potential vorticity, any deviation of the current that changes the  $f/H$  ratio, where  $f$  is the Coriolis parameter and  $H$  is the depth of the water column, will be restored.

[52] Northerly winds will drive the WSC westward into deeper water, causing a rapid change in  $H$ , with the response of the current being to move eastward to maintain a constant  $f/H$ . This will create undulations along the front which, enhanced by the horizontal velocity shear, will generate barotropic instabilities. This conceptual scheme is consistent with observations [Saloranta and Svendsen, 2001] and results from BOM (not included) that show the development of barotropic instabilities which propagate onto the shelf at times of northerly winds. Once on the shelf the pockets of Atlantic Water are topographically steered eastward along Kongsfjordrenna toward the fjord.

[53] Given that the essential requirements for the generation of the pockets of Atlantic Water are a front, sloping bathymetry and northerly winds, it is reasonable to assume that frontal instabilities will be formed year round. However, the microcat data show that Atlantic Water did not penetrate into Kongsfjorden until mid-June. The implication is that pockets of Atlantic Water residing on the shelf prior to the summer intrusion are prevented from entering the fjord by an additional control mechanism.

[54] In classic, narrow (i.e., nonrotating) fjords with a sill at the mouth acting as a partial barrier between coastal water and fjord water, exchange is usually determined by the hydraulic control of the system [Stigebrandt, 1980, 1981]. An alternate control mechanism for fjords without constrictions or sills may be geostrophic circulation of the adjacent coastal water [Klinck *et al.*, 1981]. The geostrophic current elevates or depresses the isopycnals at the fjord mouth thereby setting up pressure gradients within the fjord initiating circulation and exchange. A deep, relatively unrestricted connection between the shelf and the mouth of Kongsfjorden make it a suitable location for geostrophic control and this has been suggested in a previous review of Kongsfjorden hydrography [Svendsen *et al.*, 2002].

[55] Supporting evidence that geostrophic control is a potential mechanism restricting shelf-fjord exchange in this location comes from BOM data. Output from a 30-day model run was initialized with data from the end of May and shows pulses of Atlantic Water propagating across the shelf and following the southern boundary of Kongsfjordrenna as full-depth, topographically steered features. In the absence of any control mechanism, they would continue to follow the isobaths and enter the fjord. However, in each instance, these pulses did not penetrate the fjord but recurred away from the mouth along the north side of Kongsfjordrenna.

[56] A snapshot from the model is presented in Figure 8 and shows a pulse of Atlantic Water approaching the common mouth at a depth of 200 m. Figure 8 is a subsection of the full model domain with the east-west running Kongsfjordrenna to the left and the arms of Kongsfjorden and Krossfjorden to the right of the figure. The pulse is the pale shaded patch on the southern flank of Kongsfjordrenna having a characteristic sigma theta value of 27.95 (this value is slightly higher than defined as the boundary for AW in this paper but remains consistent with other definitions [Rudels *et al.*, 2000]). Current vectors show the flow is closely aligned with the 200-m isobath along both the southern and northern flanks. At the common mouth where the flow turns north there is a significant lateral density gradient exerting the geostrophic control

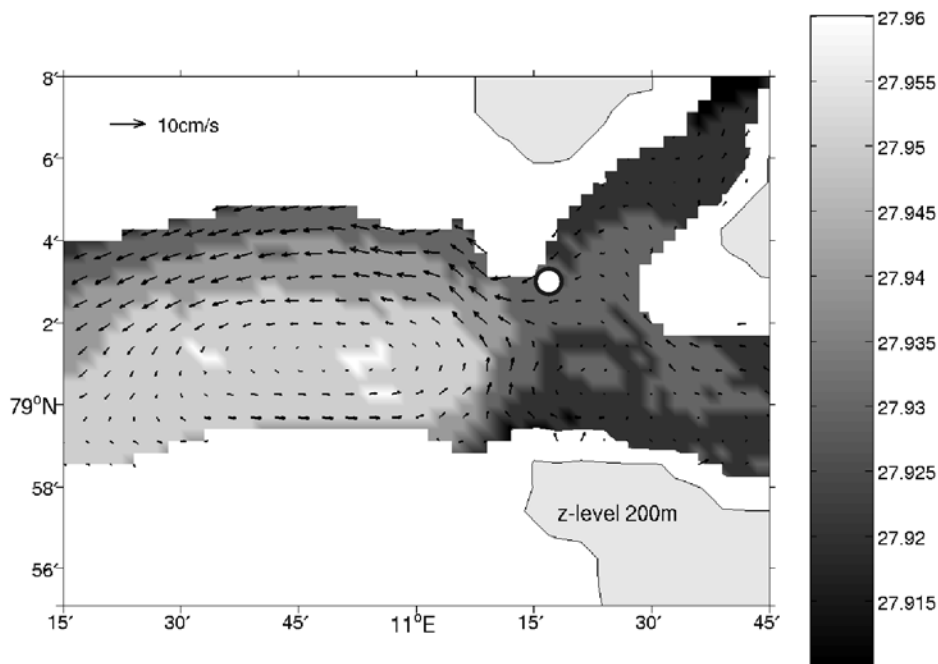


**Figure 8.** Output from a subsection of the Bergen Ocean Model for 24 June 2002 at a depth of 200 m showing the density field and current vectors. The white areas are locations in the domain that are shallower than 200 m. The coast is marked as the pale shaded region, and the mooring position is marked as the white circle.

preventing intrusion into the fjord. The region of geostrophic control does not extend across the shelf but rather is limited to the vicinity of the common mouth.

[57] To enable the pulses of Atlantic Water to enter Kongsfjorden requires that the local pressure gradient at the mouth be changed which will alter the geostrophic balance between the shelf and the fjord. The change in vertical density structure in the fjord mouth is illustrated in the bottom panels of Figures 6 and 7 which show the density recorded at the upper and lower microcats, respectively. Two principal features of the long-term changes in density during the first deployment period are: (1) a gradual decrease in density at both depths and (2) a threefold increase in the vertical density gradient.

[58] The time, and corresponding densities, marking rapid changes in temperature and salinity (indicating water mass exchange) are annotated in Figures 6 and 7 by dashed lines. We note that the upper microcat reaches a minimum sigma theta value of approximately 27.55 (13 June) and the lower microcat reaches a minimum of about 27.80 (7 June). Referring back to Figure 5, these minima in sigma theta represent typical values of AW (27.50–27.70) and TAW (27.70–27.90), respectively. The consequence of the gradual decrease in density is that ultimately there is density matching across the mouth and the lateral density gradients that support geostrophic control are diminished. When the fjord water has densities appropriately matched to those of the Atlantic Water in Kongsfjordrenna, geostrophic control is reduced and intrusions are admitted into the fjord.

[59] Further insight is gained by interpreting the hydrographic changes with reference to the prevailing meteorological conditions. Figure 9 shows a subsample of the salinity record at the lower microcat and the wind vectors

in the fjord from 1 June until the mooring was recovered. The density increase in the deep water beginning on 7 June resulted from an increase in salinity. The rate of increase was approximately  $0.015 \text{ d}^{-1}$  initially, increasing to more than  $0.05 \text{ d}^{-1}$  from 17 June onward. Figure 7 indicates that temperature also increased rapidly after the 17 June at a rate of nearly  $0.5^\circ\text{C d}^{-1}$ . These T-S changes are associated with the intrusion of ArW and then TAW. The timing of these intrusions with respect to the wind conditions is significant. Wind directions in Kongsfjorden are primarily axial and from 13 June until 22 June wind in Kongsfjorden was mostly up fjord with a mean speed of  $6 \text{ m s}^{-1}$ .

[60] The observations and analysis imply that the onset of Atlantic Water intrusion into Kongsfjorden in mid-June is linked to the coincidence of prevailing hydrographic and meteorological conditions. In summary, the conditions necessary for Atlantic Water to intrude into the Kongsfjorden-Krossfjorden system are (1) a change in the density structure of the post-winter fjord water to reduce the horizontal density gradient at the fjord mouth, (2) northerly winds to initiate cross-front exchange on the shelf, (3) propagation of Atlantic water toward the common mouth and (4) up-fjord wind to induce pycnocline readjustment leading to matching of isopycnals surfaces and breakdown of geostrophic control. Given these conditions, Atlantic Water, first TAW and then AW, will rapidly intrude into the outer basin of Kongsfjorden.

## 5.2. Distribution of AW in Kongsfjorden

[61] The CTD data in Figure 5 show clearly that by early July 2002, there had been substantial occupation by AW in the outer part of Kongsfjorden. To investigate the extent and timing of AW occupation in the inner parts of the fjord, we

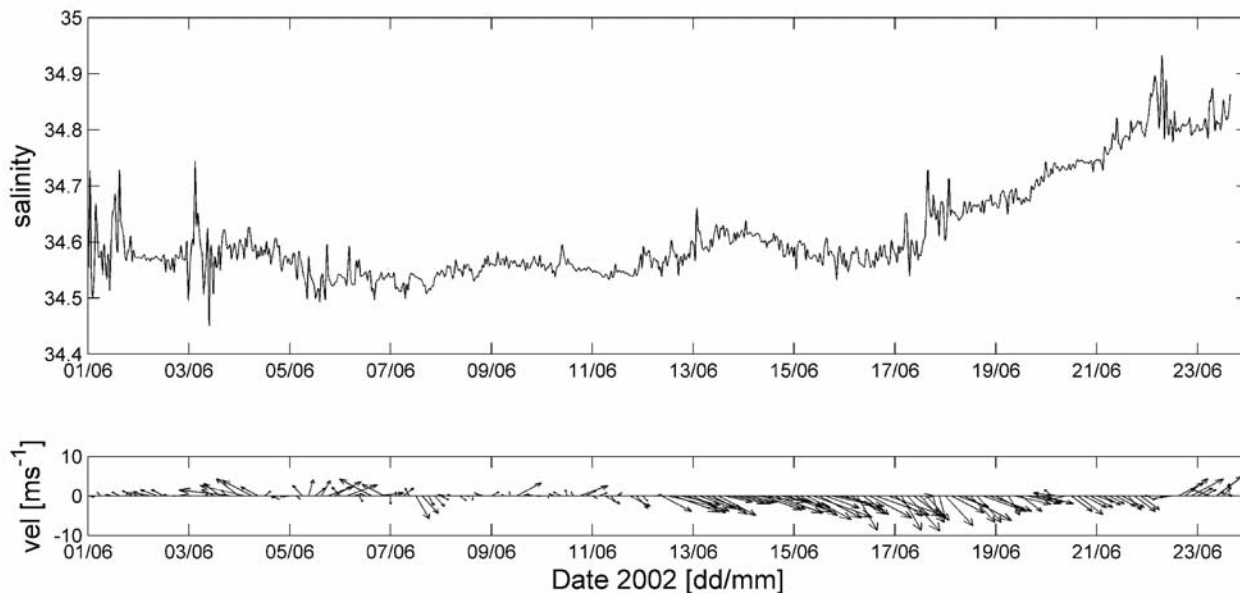


**Figure 9.** (top) Time series of salinity recorded by the lower microcat at 205 m from 1 June 2002 to 23 June 2002. (bottom) Wind vectors measured at Ny Ålesund station.

compared CTD profiles obtained in August and September of 2003 at stations K1 and K3. The data from these four profiles are plotted on the T-S diagram in Figure 10.

[62] In August 2003 there was a clear distinction between the properties of the water column at K1 and K3. The important parameters of these profiles regarding the distribution of water masses have been quantified and are summarized in Table 4. Of particular note are the difference in the thickness of the AW layer at each station and the change in thickness of the SW layer, which conforms to a

wedge shape, becoming progressively thicker toward the head of the fjord.

[63] In the intervening period between CTD profiles in August and September, AW penetrated farther into the fjord. By September, the AW occupied a 45-m-thick layer at K3 with the core at 69 m depth. There was also greater occupation of AW at K1 with the layer thickness increasing from 44 m to 72 m. The core of the AW was elevated by approximately 20 m at both stations between August and September.

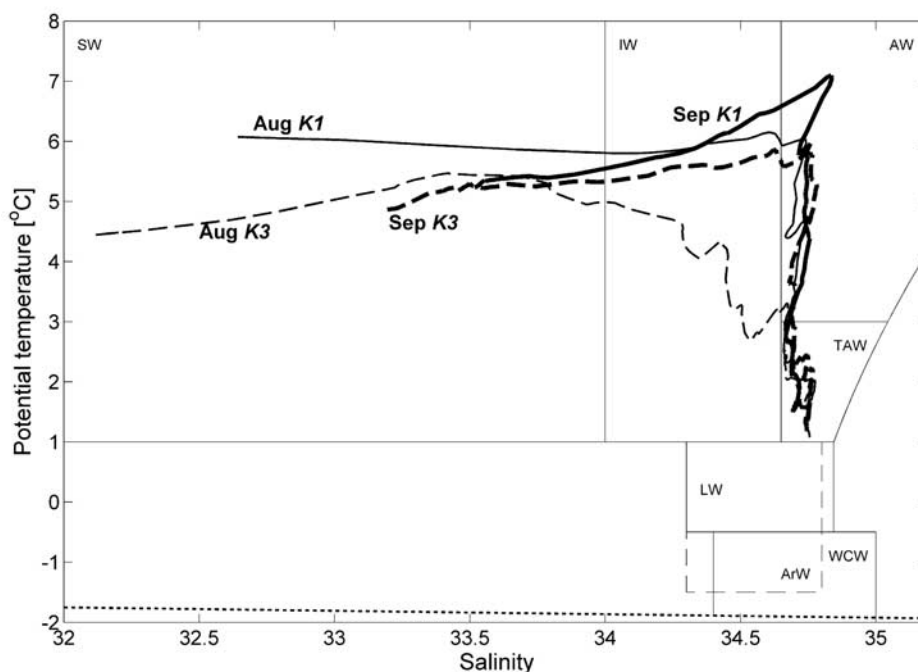


**Figure 10.** Data from CTD profiles obtained during 2003 in August (thin lines) and September (thick lines) from stations K1 (solid lines) and K3 (dashed lines) plotted on a T-S diagram.

**Table 4.** Summary of the Important Hydrographic Parameters Extracted From the CTD Profiles Obtained in August and September 2003 From Stations K1 and K3<sup>a</sup>

Month	Station	SW (S < 34.00) Z <sub>max</sub> , m	AW (S > 34.65 T > 3°C)		
			Z <sub>range</sub> , m	Z <sub>core</sub> , m	AW <sub>Zcore</sub> – SW <sub>Zmax</sub>
August	K1	21	59–103	61	40
	K3	34	89–92	90	56
September	K1	22	38–110	42	20
	K3	34	60–105	69	35

<sup>a</sup>Z<sub>max</sub> refers to the maximum observed depth for a water mass, Z<sub>range</sub> indicates the depth range at which the water mass is present, and Z<sub>core</sub> is the depth at which the water mass has the most distinct T and S signature.

[64] Another significant contrast between stations K1 and K3 is in the parameter AW<sub>Zcore</sub> – SW<sub>Zmax</sub>, the distance from the bottom of the SW layer to the AW core. In September the transition from SW to AW occurs over 20 m at K1 creating a rather strong halocline, whereas at K3 the transition occurs over 35 m and with a weaker halocline and a reduced T-S maximum for the AW core; refer to Figure 10. Conceptually, the AW intrudes into the fjord beneath the SW flowing out of the fjord. Enhanced mixing between the two water masses through shear at their interface will tend to lead to a weaker halocline as the penetration of AW extends into the fjord toward K3. Although we cannot determine any timescales for the development of AW occupation in Kongsfjorden, it is clear that there is progressive occupation of the fjord by AW during the summer months.

[65] It is interesting to note that the thickness of the SW layer at each station was exactly the same between August and September. This similarity is probably fortuitous rather than any indication of a steady state condition given that the freshwater input and distribution was not constant in time. This dynamic nature of the SW layer is seen in Figure 6 where the salinity record of the upper microcat shows rapid oscillations during August and September. Figure 11 is a north-south salinity section across the common mouth and close to the mooring from 28 September 2002 and shows that the microcat at 40 m is sited in the middle of the halocline separating the SW from AW. At that depth horizontal salinity gradients are rather weak ( $O 10^{-5} m^{-1}$ ) requiring a horizontal velocity of about  $1 m s^{-1}$  to produce the observed rate of salinity change. Current speeds measured by the ADCP peak at  $25 cm s^{-1}$  thereby ruling out horizontal advection as a likely cause. Further, vertical mixing is an unlikely cause for the rapid salinity oscillations based on a simple linear mixing model and dimensional arguments requiring a very large vertical diffusivity  $K_z$  of order  $10^{-2} m^2 s^{-1}$ .

[66] A more likely explanation for the observed rapid changes in salinity is through a vertical displacement of the halocline in response to wind forcing. Previous studies have shown that down-fjord winds can induce changes in the vertical salinity distribution in Kongsfjorden [Ingvaldsen *et al.*, 2001]. Under these conditions, Ekman transport toward the north side and consequent downwelling causes accumulation of low salinity water and a deepening of the halocline. This response is also consistent with results from a two-layer model of a wide fjord where the response to longitudinal wind is simultaneous upwelling and downwelling [Cushman-Roisin *et al.*, 1994].

[67] To investigate this further, the rate of change of salinity recorded at the upper microcat was correlated with

the down-fjord component of velocity in the period 14 August to 20 September. A maximum correlation of  $r = 0.4$  at 98% significance level was found with the salinity change lagging the wind by 3 days. This is indicative that the rapid changes in salinity observed in the upper water column are most likely caused by adjustment of the halocline in response to down-fjord winds.

[68] One final observation of the 2003 summer CTD profiles is that the deep water at K1 is colder in September than in August with T-S characteristics of matching those of deep water at K3 in August. This observation suggests a three-layer flow in Kongsfjorden during times of AW penetration. As the AW flows into the fjord at mid-depth, mass balance is maintained by enhanced SW flowing out of the fjord and flow of deep water (mainly TAW) from the

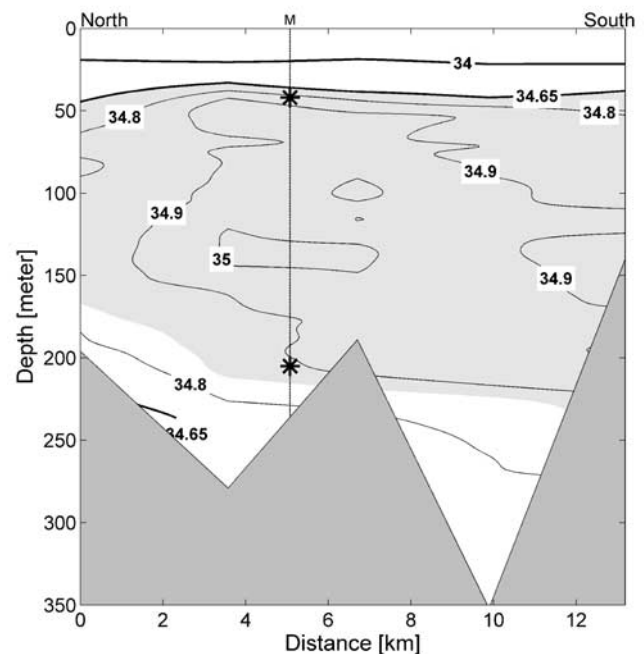


**Figure 11.** Salinity section collected in September 2002 along a north-to-south line across the common mouth of Kongsfjorden-Krossfjorden and close to the mooring location. The stations for this section are indicated in Figure 1b. The positions of the microcats are indicated in the figure by asterisks, and the pale gray shaded region is the boundary of AW occupation. Isohalines are drawn at 34.00, 34.65, and 34.8 to 35.0 in 0.1 steps, and heavy isohalines correspond to boundaries between water masses.

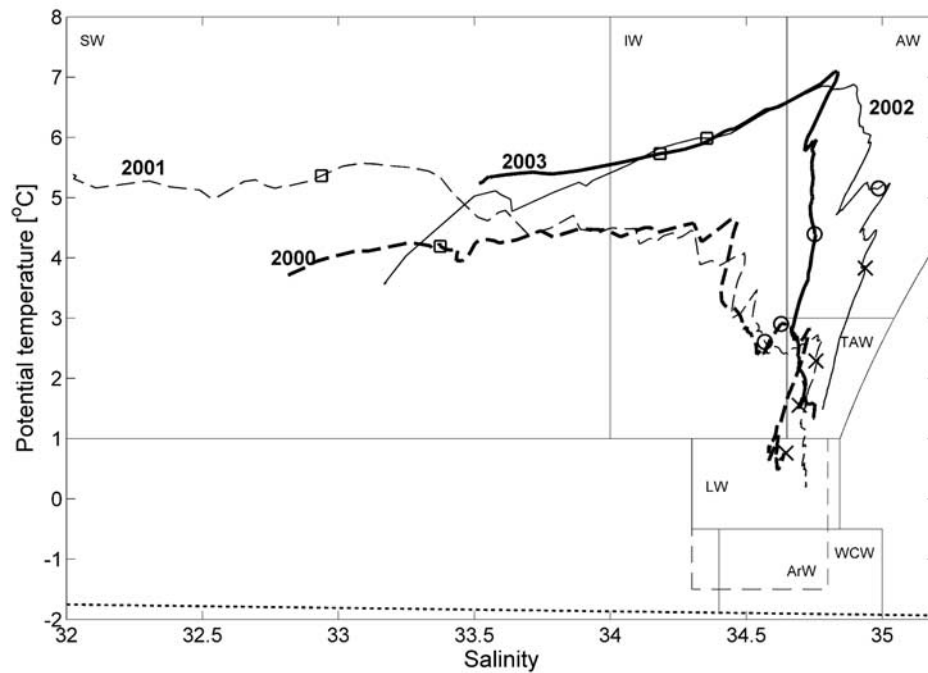


**Figure 12.** Data from CTD profiles obtained at station K1 in September from four consecutive years, 2000–2003. September 2000 (thick dashed line), 2001 (thin dashed line), 2002 (thin solid line), and 2003 (thick solid line). Depth indicators are marked at 25 m (open square), 100 m (open circle), and 200 m (cross).

inner basins toward the fjord mouth. Additional evidence for three-layer flow is found in the lower microcat record of Figure 7. From late August there are instances of rapid cooling accompanied by a decrease in salinity such that for short periods the water is more like LW in signature. This is interpreted as leakage of deep water from the inner fjord with a T-S character similar to that of LW.

### 5.3. Interannual Variations

[69] Svendsen and others [Svendsen *et al.*, 2002] gave the first indication of interannual variation in Kongsfjorden and shelf region by identifying the occurrence of Atlantic Water in the fjord each summer between 1996 and 2000. From these, they concluded that there was significant variability in the degree to which Atlantic Water occupied the fjord. Here we use CTD profiles taken at station K1 each September from 2000–2003 to derive quantitative evidence that there are strong inter-annual variations in the occurrence of Atlantic Water. These data are plotted in Figure 12, and the important parameters are summarized in Table 5.

[70] Perhaps the most remarkable aspect of this data is the similarity between two pairs of years (2000/2001 and 2002/2003) despite the substantial dynamic variability of the fjord on short timescales. Similarity is seen in both the actual water masses that are present and in their vertical distribution. In 2000 and 2001, there was complete absence of AW while TAW was restricted to depths greater than 100 m. Significantly, in these two years, the bottom of the SW layer is relatively deep at almost 50 m. The hydrography in these years could be described as being weakly Atlantic. Data from 2002 and 2003 show quite different characteristics with AW occupying most of the mid-water layer up to a depth of about 30 m. Above the AW is IW capped by a relatively thin layer ( $\sim 20$  m) of SW. The hydrography in these two years is more strongly Atlantic and a simple calculation shows that the mean vertically integrated heat content over the upper 180 m is 35% greater in the years 2002/2003 compared to 2000/2001.

[71] Further evidence for weak occupation by Atlantic Water in 2000, and also in 1999, is derived from undulating CTD surveys of Kongsfjorden in July 1999 and 2000

**Table 5.** Summary of the Important Hydrographic Parameters Extracted From the CTD Profiles Obtained at Station K1 in September 2000–2003<sup>a</sup>

Year	CTD Depth, m	$Z_{\max}$ SW ( $S < 34.00$ )	Atlantic Water ( $S > 34.65$ ) $Z_{\min}$	Atlantic Water	
				$T_{\max}$ , °C	$S_{\max}$
2000	180	47	104	2.83	34.73
2001	344	44	120	2.61	34.78
2002	333	19	30	6.88	35.03
2003	273	21	38	7.09	34.83

<sup>a</sup> $Z_{\max}$  and  $Z_{\min}$  refer to maximum and minimum depth that a water mass occupies,  $T_{\max}$  and  $S_{\max}$  are the maximum temperatures and salinities recorded in the profile – indicative of the ‘quality’ of Atlantic Water.



[Svendsen *et al.*, 2002, Figure 16]. In 1999, at depths greater than 100 m, they found the fjord to be fully occupied by TAW, contrasting with July 2000 when there was only patchy occupation of the deep water by TAW. AW was not observed in the fjord during either of these CTD surveys. Our data have shown that Kongsfjorden has a tendency to flip rapidly from an Arctic state (dominated by modified WCW and ArW) to an Atlantic state (dominated by TAW and AW) in June and July. Therefore it is unlikely that the patchy occupation by TAW observed in July 2000 would have been maintained throughout the summer. This assertion of substantial and rapid change in hydrography occurring during the summer months is substantiated by the CTD profile from September 2000 in Figure 12. At station K1 in September 2000, TAW occupied deep water below 100 m with a total absence of AW. This vertical distribution of water masses is similar to that reported by Svendsen and others [Svendsen *et al.*, 2002] for July 1999 implying that both years experienced weak occupation by Atlantic Water in the form of TAW. Further, this interpretation of a weakly Atlantic situation in 1999 and 2000 is supported by extensive CTD surveys of the shelf in 1999 and 2000 [Saloranta and Svendsen, 2001]. They reported patchy remnants of Atlantic water on the shelf rather than extensive occupation by AW observed in Figure 4 for September 2002.

[72] The data presented in Figure 12 suggest that by September, the hydrography reaches some sort of quasi steady state in a mode that is either weakly or strongly dominated by Atlantic Water; TAW or AW dominant. While there may be other hydrographic modes that are established in Kongsfjorden, the concept of “warm” or “cold” years related to interannual variation in the influence of Atlantic Water has been observed at a regional scale in the Barents Sea [Furevik, 2001] and at a local scale with reference to changes in the marine ecosystems structure in Svalbard fjords [Weslawski and Adamski, 1987].

[73] In speculating on what factors may determine whether a “warm” or “cold” year is attained, it is worth considering parameters that are internal or external to the fjord. Internal parameters include the wind vector, volume of freshwater run-off and volume of sea ice formation. Owing to the strong pycnocline and de-coupling of the surface waters, it is unlikely that fjord winds alone will influence the hydrography significantly. From Table 5, there does appear to be some simple correlation between the freshwater volume (SW layer depth) and a system that is weakly Atlantic. The volume of freshwater and its distribution across the fjord may be related to the meteorological conditions experienced in a particular year.

[74] A potential determinant of the hydrographic mode is the T-S properties of the fjord in spring, which is linked to the formation of sea ice during the preceding winter. During a particularly heavy sea ice year there will be a greater volume of WCW produced, which then may act as a buffer to the intrusion of Atlantic water. Further, given the relatively massive heat content of AW, the amount of sea ice formed during winter may itself be determined as much by the occupation of the fjord by AW as by the magnitude of the heat fluxes at the surface. In this sense, the fjord would experience some form of self-regulation based on annual preconditioning. At this stage, the influence of sea ice formation on Atlantic Water occupation remains speculative.

[75] Clearly, the most likely factors external to the fjord that may determine its hydrographic mode include the flux of AW in the WSC and the shelf wind field. Although the northward transport of AW has been shown to vary [Fahrbach *et al.*, 2001; Saloranta and Haugan, 2001; Schauer *et al.*, 2004] the variation may be insignificant in terms of the conditions experienced in Kongsfjorden. Perhaps the most likely external factor, as suggested by output from BOM for this region, are the wind vectors during the summer months creating instabilities at the shelf front. Since this ultimately provides the source of AW to the fjord, it would be useful to compare the relative influence of these internal and external factors.

## 6. Conclusions

[76] A suite of data from CTD stations and moored instruments collected in the shelf area of northwest Spitsbergen over a period of four years has been presented. The principal observation described in this paper is the massive and rapid shift in the hydrography of Kongsfjorden and on the adjacent shelf during summer 2002. The observed shift is from cold and rather saline conditions in April to warm and saline conditions in September through extensive occupation of the shelf and fjord waters by Atlantic Water. The source of Atlantic Water is the WSC running northward to the Arctic.

[77] Results from a model of the fjord and shelf system have shown that north winds induce frontal instabilities leading to pockets of Atlantic Water leaking onto the shelf. Early in the year, lateral density gradients at the mouth of the fjord exert a geostrophic control on the circulation of these pockets restricting their intrusion into the fjord. By mid-summer, modification through vertical mixing has restructured the density field at the mouth such that Atlantic Water is able to enter the fjord. At this time, further intrusion of Atlantic Water leads to the observed shift in hydrography and an increase in the heat content of the fjord and shelf waters.

[78] Our observations have confirmed the assumptions of earlier work [Svendsen *et al.*, 2002] that geostrophic control is an important mechanism in Spitsbergen fjords. More significantly, we propose that this control mechanism for shelf-fjord exchange may be common to many of the fjords connected to the Spitsbergen and Norwegian shelves. Given the appropriate combination of wind forcing, topographic steering and density structure, there may be significant cross-shelf exchange occurring along these western margins.

[79] The most far-reaching aspect of this work is probably the interaction of topographically steered currents with wind forcing to initiate frontal instabilities and exchange. Recent work on the latitudinal cooling of the WSC [Saloranta and Haugan, 2004] has concluded that lateral exchange with colder adjacent waters is necessary to account for the observed changes in subsurface heat content of the WSC. Assuming that the cross-shelf exchange mechanism that we have described in this paper acts along much of the WSS, it may prove to be an important process in modifying the heat transport to the Arctic Ocean. The integrated effect of exchange along the entire shelf area on northward heat transport needs to be quantified.

[80] The magnitude of lateral heat loss from the WSC is associated with the extent to which Atlantic Water dominates the shelf and fjord in summer. This work has demonstrated that the fjord waters show distinct interannual variability in their heat content giving rise to the concept of “warm” and “cold” years. However, we have been unable to determine the key parameters controlling the variability within the scope of this paper. We have speculated on parameters external to the shelf and fjord (AW transport and wind forcing) and internal (sea ice formation and freshwater budget), and determining the role and importance of these in controlling the magnitude of Atlantic Water occupation of the fjord merits further investigation. Sediment deposits from Kongsfjorden and the shelf will yield a record of the decadal changes in the hydrography of the region and, by extrapolation, heat transport through the Nordic Seas. This work has furthered our understanding of the present-day exchanges and will enable a more thorough interpretation of these palaeo records.

[81] **Acknowledgments.** The majority of this work was funded by (1) UK Natural Environment Research Council through SAMS Northern Seas Program (2) European project OARRE EVK3-CT1999-00002 and (3) European LSF grant NP-62/2002. The authors benefited greatly in the production of this paper through funding from The Royal Society through a European Joint Project grant and from the UHI Millennium Institute. The authors would like to thank the masters, crews and PSOs of the many research cruises that contributed to the mooring and CTD operations. We would also like to thank Simon Josey of Southampton Oceanography Centre for making the surface heat flux data available and the Alfred Wegener Institute for access to meteorological data from Koldewey Station. This manuscript benefited greatly from the comments received from two anonymous reviewers.

## References

- Basedow, S. L., K. Eiane, V. Tverberg, and M. Spindler (2004), Advection of zooplankton in an Arctic fjord (Kongsfjord, Svalbard), *Estuarine Coastal Shelf Sci.*, **60**, 113–124.
- Berntsen, J. (2000), Users guide for a modesplit sigma-coordinate numerical ocean model, version 1.0, report, Dep. of Appl. Math., Univ. of Bergen, Bergen, Norway.
- Cisewski, B., G. Budéus, and G. Krause (2003), Absolute transport estimates of total and individual water masses in the northern Greenland Sea derived from hydrographic and acoustic Doppler current profiler measurements, *J. Geophys. Res.*, **108**(C9), 3298, doi:10.1029/2002JC001530.
- Cushman-Roisin, B., L. Asplin, and H. Svendsen (1994), Upwelling in broad fjords, *Cont. Shelf Res.*, **14**(55), 1701–1721.
- Fahrbach, E., J. Meincke, S. Østerhus, G. Rohardt, U. Schauer, V. Tverberg, and J. Verduin (2001), Direct measurements of volume transports through Fram Strait, *Polar Res.*, **20**(2), 217–224.
- Fer, I., R. Skogseth, P. M. Haugan, and P. Jaccard (2003), Observations of the Storfjorden overflow, *Deep Sea Res., Part I*, **50**(10–11), 1283–1303.
- Furevik, T. (2001), Annual and interannual variability of Atlantic Water temperatures in the Norwegian and Barents Seas: 1980–1996, *Deep Sea Res., Part I*, **48**(2), 383–404.
- Haarpaintner, J., J.-C. Gascard, and P. M. Haugan (2001a), Ice production and brine formation in Storfjorden, Svalbard, *J. Geophys. Res.*, **106**(C7), 14,001–14,013.
- Haarpaintner, J., J. O’Dwyer, J.-C. Gascard, P. M. Haugan, U. Schauer, and S. Østerhus (2001b), Seasonal transformation of water masses, circulation and brine formation observed in Storfjorden, Svalbard, *Ann. Glaciol.*, **33**, 437–443.
- Hop, H., et al. (2002), The marine ecosystem of Kongsfjorden, Svalbard, *Polar Res.*, **21**(1), 167–208.
- Howe, J. A., S. G. Moreton, C. Morri, and P. Morris (2003), Multibeam bathymetry and the depositional environment of Kongsfjorden and Krossfjorden, western Spitsbergen, Svalbard, *Polar Res.*, **22**(2), 301–316.
- Ingvaldsen, R., M. B. Reitan, H. Svendsen, and L. Asplin (2001), The upper layer circulation in the Kongsfjorden and Krossfjorden—A complex fjord system on the west coast of Spitsbergen, *Mem. Natl. Inst. Polar Res. Spec. Issue Jpn.*, **54**, 393–407.
- Ito, H., and S. Kudoh (1997), Characteristics of water in Kongsfjorden, Svalbard, paper presented at NIPR Symposium on Polar Meteorology and Glaciology, Nat. Inst. of Polar Res., Tokyo.
- Josey, S. A., E. C. Kent, and P. K. Taylor (1999), New insights into the ocean heat budget closure problem from analysis of the SOC Air-Sea Flux Climatology, *J. Clim.*, **12**(9), 2856–2880.
- Klinck, J. M., J. J. O’Brien, and H. Svendsen (1981), A simple model of fjord and coastal circulation interaction, *J. Phys. Oceanogr.*, **11**, 1612–1626.
- Knutsen, Ø. (2003), Virkning av topografisk styring, vind og tidevann på sirkulasjon og utveksling av vannmasser på sokkelen til Vest-Spitsbergen., Masters thesis, Univ. of Bergen, Bergen, Norway.
- Koç, N., D. Klitgaard-Kristensen, K. Hasle, C. F. Forsberg, and A. Solheim (2002), Late glacial palaeoceanography of Hinlopen Strait, northern Svalbard, *Polar Res.*, **21**(2), 307–314.
- Kwasniewski, S., H. Hop, S. Falk-Petersen, and G. Pedersen (2003), Distribution of Calanus species in Kongsfjorden, a glacial fjord in Svalbard, *J. Plankton Res.*, **25**(1), 1–20.
- Manley, T. O. (1995), Branching of the Atlantic Water within the Greenland-Spitsbergen Passage: An estimate of recirculation, *J. Geophys. Res.*, **100**(C10), 20,627–20,634.
- Martinsen, E. A., and H. Engedahl (1987), Implementation and testing of a lateral boundary scheme as an open boundary condition in a barotropic ocean model, *Coastal Eng.*, **11**, 603–627.
- Meredith, M., K. J. Heywood, P. Dennis, L. Goldson, R. White, E. Fahrbach, U. Schauer, and S. Østerhus (2001), Freshwater fluxes through the western Fram Strait, *Geophys. Res. Lett.*, **28**(8), 1615–1618.
- Quadfasel, D., B. Rudels, and K. Kurz (1988), Outflow of dense water from a Svalbard fjord into the Fram Strait, *Deep Sea Res.*, **35**(7), 1143–1150.
- Rudels, B., R. Meyer, E. Fahrbach, V. V. Ivanov, S. Østerhus, D. Quadfasel, U. Schauer, V. Tverberg, and R. A. Woodgate (2000), Water mass distribution in Fram Strait and over the Yermak Plateau in summer 1997, *Ann. Geophys.*, **18**, 687–705.
- Saloranta, T. M., and P. M. Haugan (2001), Interannual variability in the hydrography of Atlantic water northwest of Svalbard, *J. Geophys. Res.*, **106**(C7), 13,931–13,943.
- Saloranta, T. M., and P. M. Haugan (2004), Northward cooling and freshening of the warm core of the West Spitsbergen Current, *Polar Res.*, **23**(2), 79–88.
- Saloranta, T. M., and H. Svendsen (2001), Across the Arctic front west of Spitsbergen: High-resolution CTD sections from 1998–2000, *Polar Res.*, **20**(2), 177–184.
- Schauer, U., E. Fahrbach, S. Østerhus, and G. Rohardt (2004), Arctic warming through the Fram Strait: Oceanic heat transport from 3 years of measurements, *J. Geophys. Res.*, **109**, C06026, doi:10.1029/2003JC001823.
- Skogseth, R. (2003), Dense water production processes in Storfjorden, Ph.D. thesis, Univ. Cent. on Svalbard, Longyearbyen, Norway.
- Skogseth, R., P. M. Haugan, and J. Haarpaintner (2004), Ice and brine production in Storfjorden from four winters of satellite and in situ observations and modeling, *J. Geophys. Res.*, **109**, C10008, doi:10.1029/2004JC002384.
- Souza, A. J., J. H. Simpson, M. Hari Krishnan, and J. Malarkey (2001), Flow structure and seasonality in the Hebridean slope current, *Oceanol. Acta*, **24**, S63–S76.
- Stigebrandt, A. (1980), Some aspects of tidal interaction with fjord constrictions, *Estuarine Coastal Shelf Sci.*, **11**, 151–166.
- Stigebrandt, A. (1981), A mechanism governing the estuarine circulation in deep, strongly stratified fjords, *Estuarine Coastal Shelf Sci.*, **13**, 197–211.
- Svendsen, H., et al. (2002), The physical environment of Kongsfjorden-Krossfjorden, an Arctic fjord system in Svalbard, *Polar Res.*, **21**(1), 133–166.
- Walczowski, W., J. Piechura, R. Osinski, and P. Wiczorek (2005), The West Spitsbergen Current volume and heat transport from synoptic observations in summer, *Deep Sea Res., Part I*, **52**(8), 1374–1391.
- Weslawski, J. M., and P. Adamski (1987), Warm and cold years in south Spitsbergen coastal marine ecosystem, *Pol. Polar Res.*, **8**, 96–106.

F. Cottier, C. Griffiths, and M. Inall, Scottish Association for Marine Science, Dunstaffnage Marine Laboratory, Oban PA37 1QA, UK. (fcott@sams.ac.uk)

F. Nilsen, University Centre in Svalbard (UNIS), N-9171 Longyearbyen, Svalbard, Norway.

H. Svendsen, Geophysical Institute, University of Bergen, Allegaten 70, N-5007 Bergen, Norway.

V. Tverberg, Norwegian Polar Institute, Polar Environmental Centre, N-9296 Tromsø, Norway.